World Research Journal of Civil Engineering
World Research Journal of Civil Engineering
ISSN: 2277-5986 & E-ISSN: 2277-5994, Volume 1, Issue 1, 2011, pp-07-14
Available online at http://www.bioinfo.in/contents.php?id=173

# CHARACTERISTICS OF RECENT FLOODS IN PERSIAN GULF CATCHMENT

**AKBARI G. AND FIROOZI B.**
Department of Civil Engineering, University of Sistan and Baluchestan, Zahedan, Iran
*Corresponding Author: Email- gakbari@hamoon.usb.ac.ir, behzad_frz@yahoo.com

Received: June 28, 2011; Accepted: November 03, 2011

**Abstract-** Four novel models were developed and applied to arid zone wild rivers. Floods in deserts and overland flow is complicated and almost ignored in many models, but dealt here. Contributions made for application of numerical modelling in odd hydrologic watersheds, flood wave routing and solving the governing equations of flood wave propagations. Unsteady non-uniform flow, known as the dynamic wave equations was solved applied to a difficult hydrologic case study. Equations involved in the formulation of the selected problem are highly nonlinear with having no analytical solutions. Five techniques were examined and compared for the best solutions of fully dynamic flood routing problems. Performances of explicit and implicit finite differences methods such as Lax, Mac-Cormack, Method of Characteristics and Preissmann scheme were compared with available computer software. The models developed are results of writing, compiling and running several computer programs using *MATLAB* software and available standard *HEC series* computer models.
**Key Words-** Lax, Mac-Cormack, Characteristics, Preissmann scheme, wild rivers flood, *HEC-series*

## Introduction

Understanding flood wave routing theory and solving the governing equations accurately is an important issue in advanced hydrology and hydraulics. In unsteady open channel flows, the velocities and water depths change with time and longitudinal position. For one-dimensional applications, the relevant flow parameters (e.g. *V* and *y*) are functions of time and longitudinal distance. Analytical solutions of the basic equations are nearly impossible because of their nonlinearity, but numerical techniques provide approximate solutions for some specific cases [1-5]. Flood wave propagation in overland and open channel flows may be described by the complete equations of motion for unsteady non-uniform flow, known as the *dynamic wave* equations, first proposed by Saint-Venant. These equations are highly nonlinear and therefore do not have analytical solutions. With the greatly improved speed and capacity of digital computers in recent years, dynamic routing models have been widely used for flood forecasting. However, real time observed data are seldom incorporated into the dynamic routing models to improve the accuracy of forecasting. Developing numerical models that can accurately predict surface runoff and flood routing through the channels is of interest to a wide variety of users, including city planners and irrigation practitioners. These models can also be easily extended to predict the fate and transport of contaminants along the surface and downstream. There have been numerous studies in the literature to solve the Saint-Venant equations using different numerical techniques but the application of current study differs from earlier models. In this paper comprehensive solutions of the fully Saint-Venant equations through various finite difference methods such as Lax diffusive, Mac-Cormack scheme, Preissmann scheme and Method of Characteristics for unsteady flow simulation in natural rivers are presented. This is a novel attempt toward applications for specified case studies which have not been done so far.

Flooding in the river basin and the waterways in the studied area as shown in Fig (1) is always a cause for concern? A number of branches for the River were undertaken in this investigation and available hydrometric stations were part of data used. Superabundant flood from regions located in the South-East of Iran and Northern part of Arab states were considered. Great section of this basin covered by mountainous land, but this zone is not very high. There are mound zone and plain zone in north that drown by water on spate situation. There always have been restrictions in weather stations propagation in East and South of the area that is because of countries in the region including water borders between Iran, Pakistan and Oman states in the Gulf. Therefore in this study data station's in southern part was used.

Regarding to the characteristics of the recent flooding in the area, there has not been many substantial research works reported in literatures, but similar flooding prediction reports may be referred to be [6-12].

## Governing Equations

The dynamic routing model is based on the dynamic wave theory of the Saint-Venant equations which consist of the continuity and momentum equations. For prismatic channels having no lateral inflow or outflow the continuity and momentum equations is defined as:

$$\frac{\partial y}{\partial t} + D_h \frac{\partial V}{\partial x} + V \frac{\partial y}{\partial x} = 0 \quad (1)$$

$$\frac{\partial V}{\partial t} + V \frac{\partial V}{\partial x} + g \frac{\partial y}{\partial x} = g(S_o - S_f) \quad (2)$$

In which V is flow velocity; y is flow depth; Dh = A/B is hydraulic depth; A is flow area; B is top water surface width; So is channel bottom slope; Sf is slope of the energy grade line; x is distance along the channel length; t is time; and is the acceleration due to gravity.

**Model Development and Methodology**

The continuity and momentum equations form a set of nonlinear hyperbolic partial differential equations. Numerical solutions of Eqns. (1) and (2) can be obtained if appropriate initial and boundary conditions are prescribed. Details of various numerical methods that can be used to solve the governing equations of flood wave propagation in natural rivers can be found in literature. A good introduction of these numerical methods has been given by Author in his earlier researches. In this work, the fully Saint-Venant equations are solved for a wide river with 30km length using Method of Characteristics and three types of finite difference methods. The results of these numerical solutions are compared with the *HEC-RAS* commercial computer model to verify the numerical schemes.

**Method of characteristics**

In this method by elimination of the space variable, *x*, from the governing equations we can convert them into the ordinary differential equations. The transformed equations are valid only along the characteristics. Here we have used the method of specified intervals to calculate the velocity and depth in advanced time step. To use specified intervals, interpolations become necessary either in time or in space, since all characteristics do not pass through the grid points. In this method, the size of the spatial and time grids has been specified.

**Lax diffusive scheme**

In this scheme the partial derivatives and other variables are approximated as follows:

$$\frac{\partial f}{\partial x} = \frac{f_{i+1}^k - f_{i-1}^k}{2\Delta x}$$

$$\frac{\partial f}{\partial t} = \frac{f_i^{k+1} - f^*}{\Delta t}$$

$$f^* = \frac{1}{2}(f_{i-1}^k + f_{i+1}^k)$$

$$D^* = \frac{1}{2}(D_{i-1}^k + D_{i+1}^k)$$

$$S_f^* = \frac{1}{2}(S_{f_{i-1}}^k + S_{f_{i+1}}^k) \quad (3)$$

In which *f* are substituted for both dependent variables *y* and *V*. These approximations are used in the conservation forms of the governing equations as follows. The conservation forms of the governing equations in the matrix form may be written as

$$\boldsymbol{U}_t + \boldsymbol{F}_x + \boldsymbol{S} = 0 \quad (4)$$

In which

$$\boldsymbol{U} = \begin{pmatrix} A \\ VA \end{pmatrix}$$

$$\boldsymbol{F} = \begin{pmatrix} VA \\ V^2 A + gA\bar{y} \end{pmatrix}$$

$$\boldsymbol{S} = \begin{pmatrix} 0 \\ -gA(S_o - S_f) \end{pmatrix} \quad (5)$$

Where, $A\bar{y}$ is moment of flow area about the free surface. Friction slope is predicted using Manning's equation:

$$S_f = \frac{n^2 V^2}{R^{4/3}} \quad (6)$$

In which, *R=A/P* is hydraulic radius; *P* is wetted perimeter; and *n* is the Manning's roughness coefficient. Substitution of the finite-difference approximations of Eqn. (3) into Eqn. (4) yields

$$\boldsymbol{U}_i^{k+1} = \frac{1}{2}(\boldsymbol{U}_{i+1}^k + \boldsymbol{U}_{i-1}^k) - \frac{1}{2}\frac{\Delta t}{\Delta x}(\boldsymbol{F}_{i+1}^k - \boldsymbol{F}_{i-1}^k) - \boldsymbol{S}^* \Delta t \quad (7)$$

Eqn. (7) has been used at the interior grid points to compute the unsteady flow depth and flow velocity. At the boundaries the method of specified interval is employed here. In this way boundary equations are solved simultaneously, with the positive and/or negative characteristic equations to determine the flow conditions at the boundary nodes [4].

**McCormack scheme**

The McCormack scheme is an explicit, two-step predictor-corrector scheme that is second-order accurate in space and time. This explicit finite difference scheme has been applied for analyzing unsteady, open-channel flows.

*Predictor step*

For one-dimensional flow backward finite-differences are used to approximate the spatial partial derivatives in the predictor part

$$\frac{\partial \boldsymbol{U}}{\partial t} = \frac{\boldsymbol{U}_i^* - \boldsymbol{U}_i^k}{\Delta t} \quad (8)$$

$$\frac{\partial \boldsymbol{F}}{\partial x} = \frac{\boldsymbol{F}_i^k - \boldsymbol{F}_{i-1}^k}{\Delta x} \quad (9)$$

In which the superscript $*$ refers to variables computed during the predictor part. Substitution of these finite differences into Eq. (3) and simplification of the resulting equation yield

$$\boldsymbol{U}_i^* = \boldsymbol{U}_i^k - \frac{\Delta t}{\Delta x}(\boldsymbol{F}_i^k - \boldsymbol{F}_{i-1}^k) - \boldsymbol{S}_i^k \Delta t \quad (10)$$

The computed value of $U_i^*$ gives $A^*$ and $Q^*$, from which we determine the values of $V^*$ and $y^*$. We compute these for all the computational nodes. These values are then used in the corrector part to compute $F^*$ and $S^*$.

*Corrector step*

For one-dimensional flow forward finite-differences are used to approximate the spatial partial derivatives in the corrector part

$$\frac{\partial U}{\partial t} = \frac{U_i^{**} - U_i^k}{\Delta t} \qquad (11)$$

$$\frac{\partial F}{\partial x} = \frac{F_{i+1}^* - F_i^*}{\Delta x} \qquad (12)$$

Substituting these finite differences and $S = S_i^*$ into Eq. (3), we obtain

$$U_i^{**} = U_i^k - \frac{\Delta t}{\Delta x}(F_{i+1}^* - F_i^*) - S_i^* \Delta t \qquad (13)$$

In which the superscript $**$ refers to the values of the variables after the corrector step. The value of $\mathbf{U}_i$ at the unknown time level $k + 1$ is given by

$$U_i^{k+1} = \frac{1}{2}(U_i^* + U_i^{**}) \qquad (14)$$

In this method also at the boundaries the method of specified interval are used.

**Preissmann implicit scheme**

Several implicit finite-difference schemes have been used for the analysis of unsteady open-channel flows. The Preissmann scheme has been extensively used since the early 1960s.

In this scheme the partial derivatives and other coefficients are approximated as follows:

$$\frac{\partial f}{\partial x} = \frac{\beta(f_{i+1}^{k+1} - f_i^{k+1}) + (1-\beta)(f_{i+1}^k - f_i^k)}{\Delta x}$$

$$\frac{\partial f}{\partial t} = \frac{(f_i^{k+1} + f_{i+1}^{k+1}) - (f_i^k + f_{i+1}^k)}{\Delta x}$$

$$f = \frac{1}{2}\beta(f_{i+1}^{k+1} + f_i^{k+1}) + \frac{1}{2}(1-\beta)(f_{i+1}^k + f_i^k) \qquad (15)$$

In which $\beta$ is a weighting coefficient; $f$ refers to both $V$ and $y$ in the partial derivatives and stands for $S_f$ *and* $V$ as a coefficient.

By substituting the above finite-difference approximations and the coefficients into Eqns. (3) and rearranging the terms of the resulting equation, we obtain:

$$U_i^{k+1} + U_{i+1}^{k+1} + 2\frac{\Delta t}{\Delta x}(\beta(F_{i+1}^{k+1} - F_i^{k+1}) + (1-\beta)(F_{i+1}^k - F_i^k)) + \Delta t(\beta(S_i^{k+1} + S_{i+1}^{k+1}) + (1-\beta)(S_{i+1}^k + S_i^k)) = U_i^k + U_{i+1}^k \qquad (16)$$

By applying the Eqn. (16) for each node and the boundary conditions we have a set of nonlinear algebraic equations. Here the nonlinear system of equations has been solved by Newton Raphson method.

**Initial and boundary conditions**

Values of depth(y) and discharge (*Q*) at the beginning of the time step are to be specified at all the nodes along the channel as initial conditions. The two boundary conditions required by the model are the inflow discharge hydrograph at the upstream boundary, and the zero-depth at the downstream boundary. At the boundaries for explicit schemes we solve the positive characteristic equation simultaneously with the condition imposed by the boundary for the downstream-end condition and the negative characteristic with the upstream-end condition for the upstream boundary.

**Stability**

For the stability of the schemes, it is necessary that the Courant number, $C_n$, is less than or equal to 1, where

$$C_n = \frac{|V| \pm c}{\Delta x/\Delta t} \qquad (17)$$

Courant condition must be satisfied at each grid point during every computational interval. The preissmann scheme is unconditionally stable provided $0.5 \leq \beta \leq 1$, i.e., the flow variables are weighted towards the $k + 1$ time level.

**Application of Models**

To demonstrate the potential of the methods used in this research, models are applied to simulate flood routing problems in a wild river basin Persian Gulf area.

Flood routing in a 30 km long wild river with bed slope ($S_0$) equal to 0.00011 and channel width ($B$) equal to 120m is considered for the studied area. Uniform flow exists initially base flow ($Q_b$) $100 m^3/sec$. Friction slope is predicted using Manning's equation with roughness coefficient n equal to 0.027. The upstream discharge hydrograph is given by:

$$Q(t) = \frac{Q_p}{2} sin(\frac{\pi t}{t_p} - \frac{\pi}{2}) + \frac{Q_p}{2} + Q_b \qquad for \quad t \leq t_p$$

$$Q(t) = \frac{Q_p}{2} cos(\pi \frac{t - t_p}{t_b - t_p}) + \frac{Q_p}{2} + Q_b \qquad for \ t_p < t \leq t_b$$

$$Q(t) = Q_b \qquad for \quad t > t_b \qquad (18)$$

Where $t_b$ is the time base equal to 5 hours, $t_p$ is the time to peak equal to 15 hours and $Q_p$ is the peak discharge of hydrograph equal to 800 $m^3/sec$. The Downstream boundary condition is considered by Manning's equation:

$$Q = \frac{1}{n} A R^{2/3} S_0^{1/2} \qquad (19)$$

**Results and Discussions**

The initial condition for all of the models corresponds to uniform flow with discharge 100 $m^3/sec$ and flow depth 1.6 *m*. Also, the friction slope is computed using Manning's equation with roughness coefficient n equal to 0.027. The upstream discharge hydrograph (Eq. 18) and the downstream stage-discharge relationship (Eq. 19) are used as boundary conditions for the models. For all of models time and space interval have been considered as 120 *sec* and 1000 *m*, respectively. The weighting coefficient $\beta$ is selected as 0.6 for Preissmann scheme.

Computed unsteady flow data through numerical models at the upstream-end and at the 16km section are given in Table 1. It can be seen that the arrival time of peak flow in the all of models is equal to 7 hours. In addition, the peak flow discharges per unit width are 6.50, 6.28, 6.40, 6.40 and 6.38 $m^3s^{-1}m^{-1}$ , and the corresponding peak flow depths are 5.16, 5.14, 5.12, 5.12 and 5.11 m, computed with Method of Characteristics, Lax diffusive scheme, Mac-Cormack scheme, Preissmann scheme, and *HEC-RAS* computer model, respectively. Computed unsteady flow data through numerical models at upstream-end and at the Downstream-end are given in Table 2. It can be seen that at downstream- end, the arrival time of the peak flow in all of the numerical models is equal to 10 hours. In addition, the peak flow discharges per unit width are 5.60, 5.59, 5.53, 5.53 and 5.52 $m^3s^{-1}m^{-1}$ ,and the peak flow depths are 5.12, 5.12, 5.08, 5.08, 5.07 m, computed with Method of Characteristics, Lax diffusive scheme, Mac-Cormack scheme, Preissmann scheme, and *HEC-RAS* computer model, respectively, at downstream-end. From the results of table 1 and 2 it can be concluded that the computed unsteady flow data using Method of Characteristics model is more than other models. If we consider the *HEC RAS* computer model as a benchmark it can be concluded that the results of Preissmann and McCormack schemes are better than the other numerical methods that have been used in this research. Stage and discharge hydrographs obtained at a section distant 15 km from the upstream end and at the downstream end of the channel by applying all of the models are shown in Fig. (2).

**Conclusion**

In this research the solution of complete Saint-Venant equations (continuity and momentum equations) was applied to a wild river basin area. Flood routing problems in a wide river through different explicit and implicit numerical schemes and *HEC-RAS* computer model was presented. It was seen that there is good agreement among the results of the Method of Characteristics, Lax diffusive scheme, McCormack scheme and Preissmann scheme. In addition, the results of these models agree well with those of *HEC-RAS* model. These numerical methods have not been employed and verified for such an odd river basin area.

**References**


[1] Abbott M.B. (1979) *"Computational Hydraulics." Pitman: London.*

[2] Akbari G.H. (2007) *J. Proceedings of the Institution of Civil Engineering. ice.,* 153-158.

[3] Akbari G.H. (2011) *"Development of numerical mathematical models for optimization of conveyance factor for water and sediment transport in Saravan water shed are", a research project submitted to local water authorities, Zahedan Iran.*

[4] Chaudhry M.H. (1993) *Open-channel Flow," Prentice-Hall: Englewood Cliffs, NJ.*

[5] Chau K.W. (2006) *Journal of Hydrology,* Vol. 329, No. 3-4, pp. 363-367.

[6] Cheng C.T., Wu X.Y. and Chau K.W. (2005) *Hydrological Sciences Journal,* Vol. 50, No. 6, pp. 1069-1087

[7] Engineering Manual (1994) *Flood-Runoff Analysis, Department of the Army U.S. Army Corps of Engineers Washington* DC 20314-1000.

[8] Lin J.Y., Cheng C.T. and Chau K.W. (2006) *Hydrological Sciences Journal,* Vol. 51, No. 4, pp. 599-612.

[9] Wu C.L., Chau K.W. and Li Y.S. (2009) *Water Resources Research,* 45, W08432, doi: 10.1029/2007WR006737.

[10] Moramarco T., Pandolfo C. and Singh V.P. (2008) *J. Hydro.,* 13(11), 1078-1088.

[11] Srinivasulu S. and Jain A. (2009) *J. Hydro.,* 14(1), 75-83.

[12] US Army Corps of Engineers (2008*) HEC-RAS User's Manual"* version 4.

*Table 1 measured stage and discharge hydrograph at 16km section using all of the models*

| Upstream-end | | | | | | | 15km from upstream | | | | | |
|---|---|---|---|---|---|---|---|---|---|---|---|---|
| Characteristics | | | Lax diffusive | | Mac-Cormack | | Preissmann | | *HEC-RAS* | | | |
| Time (h) | *q=Q/B* ($m^3s^{-1}m^{-1}$) | Stage (m) | *q=Q/B* ($m^3s^{-1}m^{-1}$) | Stage (m) | *q=Q/B* ($m^3s^{-1}m^{-1}$) | Stage (m) | *q=Q/B* ($m^3s^{-1}m^{-1}$) | Stage (m) | *q=Q/B* ($m^3s^{-1}m^{-1}$) | Stage (m) | *q=Q/B* ($m^3s^{-1}m^{-1}$) | Stage (m) |
| 0 | 0.83 | 1.6 | 0.83 | 1.6 | 0.83 | 1.6 | 0.83 | 1.6 | 0.83 | 1.6 | 0.83 | 1.6 |
| 1 | 1.45 | 1.89 | 0.83 | 1.6 | 0.84 | 1.6 | 0.83 | 1.6 | 0.83 | 1.6 | 0.84 | 1.6 |
| 2 | 3.11 | 2.76 | 0.88 | 1.62 | 0.98 | 1.68 | 0.87 | 1.62 | 0.87 | 1.61 | 0.88 | 1.62 |
| 3 | 5.17 | 3.8 | 1.3 | 1.83 | 1.63 | 2.06 | 1.3 | 1.84 | 1.3 | 1.83 | 1.33 | 1.85 |
| 4 | 6.85 | 4.68 | 2.88 | 2.63 | 3.14 | 2.86 | 2.88 | 2.64 | 2.87 | 2.63 | 2.9 | 2.65 |
| 5 | 7.5 | 5.22 | 4.94 | 3.69 | 4.89 | 3.77 | 4.87 | 3.67 | 4.85 | 3.66 | 4.85 | 3.67 |
| 6 | 7.34 | 5.43 | 6.13 | 4.45 | 5.95 | 4.45 | 6.04 | 4.41 | 6.02 | 4.4 | 6.01 | 4.4 |
| 7 | 6.87 | 5.46 | 6.5 | 4.88 | 6.28 | 4.86 | 6.4 | 4.83 | 6.4 | 4.82 | 6.38 | 4.82 |
| 8 | 6.14 | 5.34 | 6.36 | 5.1 | 6.17 | 5.09 | 6.27 | 5.05 | 6.27 | 5.05 | 6.26 | 5.04 |
| 9 | 5.21 | 5.09 | 5.94 | 5.16 | 5.8 | 5.14 | 5.86 | 5.12 | 5.86 | 5.12 | 5.85 | 5.11 |
| 10 | 4.18 | 4.74 | 5.35 | 5.08 | 5.24 | 5.04 | 5.28 | 5.03 | 5.29 | 5.04 | 5.28 | 5.03 |
| 11 | 3.15 | 4.31 | 4.67 | 4.88 | 4.57 | 4.82 | 4.61 | 4.83 | 4.62 | 4.84 | 4.61 | 4.83 |
| 12 | 2.22 | 3.82 | 3.96 | 4.59 | 3.86 | 4.51 | 3.91 | 4.54 | 3.92 | 4.55 | 3.91 | 4.54 |
| 13 | 1.48 | 3.32 | 3.29 | 4.25 | 3.18 | 4.14 | 3.24 | 4.19 | 3.25 | 4.2 | 3.25 | 4.19 |
| 14 | 1 | 2.85 | 2.71 | 3.88 | 2.59 | 3.74 | 2.67 | 3.83 | 2.67 | 3.83 | 2.67 | 3.83 |
| 15 | 0.83 | 2.48 | 2.25 | 3.53 | 2.13 | 3.37 | 2.21 | 3.47 | 2.22 | 3.47 | 2.22 | 3.47 |
| 16 | 0.83 | 2.24 | 1.94 | 3.21 | 1.82 | 3.04 | 1.9 | 3.16 | 1.9 | 3.16 | 1.9 | 3.16 |
| 17 | 0.83 | 2.06 | 1.71 | 2.94 | 1.61 | 2.77 | 1.68 | 2.89 | 1.69 | 2.9 | 1.69 | 2.89 |
| 18 | 0.83 | 1.93 | 1.54 | 2.72 | 1.44 | 2.54 | 1.52 | 2.67 | 1.52 | 2.67 | 1.52 | 2.67 |
| 19 | 0.83 | 1.84 | 1.4 | 2.53 | 1.32 | 2.36 | 1.38 | 2.49 | 1.38 | 2.49 | 1.38 | 2.49 |
| 20 | 0.83 | 1.78 | 1.29 | 2.36 | 1.22 | 2.22 | 1.27 | 2.33 | 1.27 | 2.33 | 1.27 | 2.33 |
| 21 | 0.83 | 1.73 | 1.2 | 2.23 | 1.14 | 2.1 | 1.18 | 2.2 | 1.18 | 2.2 | 1.19 | 2.2 |
| 22 | 0.83 | 1.69 | 1.13 | 2.11 | 1.08 | 2 | 1.11 | 2.09 | 1.11 | 2.09 | 1.11 | 2.09 |
| 23 | 0.83 | 1.67 | 1.07 | 2.02 | 1.03 | 1.93 | 1.06 | 2 | 1.06 | 2 | 1.06 | 2 |
| 24 | 0.83 | 1.65 | 1.02 | 1.94 | 0.99 | 1.86 | 1.01 | 1.92 | 1.01 | 1.92 | 1.01 | 1.92 |
| 25 | 0.83 | 1.64 | 0.98 | 1.87 | 0.96 | 1.81 | 0.97 | 1.86 | 0.97 | 1.86 | 0.97 | 1.86 |
| 26 | 0.83 | 1.63 | 0.95 | 1.82 | 0.94 | 1.77 | 0.94 | 1.81 | 0.94 | 1.81 | 0.94 | 1.81 |
| 27 | 0.83 | 1.62 | 0.92 | 1.77 | 0.92 | 1.74 | 0.92 | 1.77 | 0.92 | 1.77 | 0.92 | 1.76 |
| 28 | 0.83 | 1.61 | 0.9 | 1.74 | 0.9 | 1.71 | 0.9 | 1.73 | 0.9 | 1.73 | 0.9 | 1.73 |
| 29 | 0.83 | 1.61 | 0.89 | 1.71 | 0.89 | 1.69 | 0.89 | 1.7 | 0.89 | 1.7 | 0.89 | 1.7 |
| 30 | 0.83 | 1.61 | 0.88 | 1.69 | 0.88 | 1.67 | 0.87 | 1.68 | 0.87 | 1.68 | 0.87 | 1.68 |
| 31 | 0.83 | 1.61 | 0.87 | 1.67 | 0.87 | 1.66 | 0.87 | 1.67 | 0.87 | 1.66 | 0.87 | 1.66 |
| 32 | 0.83 | 1.6 | 0.86 | 1.65 | 0.86 | 1.65 | 0.86 | 1.65 | 0.86 | 1.65 | 0.86 | 1.65 |
| 33 | 0.83 | 1.6 | 0.85 | 1.64 | 0.86 | 1.64 | 0.85 | 1.64 | 0.85 | 1.64 | 0.85 | 1.64 |
| 34 | 0.83 | 1.6 | 0.85 | 1.63 | 0.85 | 1.63 | 0.85 | 1.63 | 0.85 | 1.63 | 0.85 | 1.63 |
| 35 | 0.83 | 1.6 | 0.85 | 1.63 | 0.85 | 1.63 | 0.85 | 1.62 | 0.85 | 1.62 | 0.85 | 1.62 |

*Table 2 measured stage and discharge hydrograph at Downstream-end using all of the models*

| Upstream-end | | | | | | 15km from upstream | | | | | | |
|---|---|---|---|---|---|---|---|---|---|---|---|---|
| Characteristics | | | Lax diffusive | | Mac-Cormack | | Preissmann | | *HEC-RAS* | | | |
| Time (h) | *q=Q/B* ($m^3s^{-1}m^{-1}$) | Stage (m) | *q=Q/B* ($m^3s^{-1}m^{-1}$) | Stage (m) | *q=Q/B* ($m^3s^{-1}m^{-1}$) | Stage (m) | *q=Q/B* ($m^3s^{-1}m^{-1}$) | Stage (m) | *q=Q/B* ($m^3s^{-1}m^{-1}$) | Stage (m) | *q=Q/B* ($m^3s^{-1}m^{-1}$) | Stage (m) |
| 0 | 0.83 | 1.60 | 0.83 | 1.60 | 0.83 | 1.60 | 0.83 | 1.60 | 0.83 | 1.60 | 0.84 | 1.60 |
| 1 | 1.45 | 1.89 | 0.83 | 1.60 | 0.83 | 1.60 | 0.83 | 1.60 | 0.83 | 1.60 | 0.84 | 1.60 |
| 2 | 3.11 | 2.76 | 0.83 | 1.60 | 0.83 | 1.60 | 0.83 | 1.60 | 0.83 | 1.60 | 0.84 | 1.60 |
| 3 | 5.17 | 3.80 | 0.83 | 1.60 | 0.86 | 1.63 | 0.83 | 1.60 | 0.83 | 1.60 | 0.84 | 1.60 |
| 4 | 6.85 | 4.68 | 0.86 | 1.63 | 1.02 | 1.80 | 0.86 | 1.63 | 0.86 | 1.62 | 0.86 | 1.63 |
| 5 | 7.50 | 5.22 | 1.09 | 1.89 | 1.61 | 2.39 | 1.10 | 1.89 | 1.09 | 1.88 | 1.13 | 1.92 |
| 6 | 7.34 | 5.43 | 2.21 | 2.89 | 2.87 | 3.40 | 2.22 | 2.90 | 2.24 | 2.92 | 2.27 | 2.94 |
| 7 | 6.87 | 5.46 | 3.80 | 4.03 | 4.20 | 4.29 | 3.78 | 4.02 | 3.79 | 4.03 | 3.79 | 4.03 |
| 8 | 6.14 | 5.34 | 4.89 | 4.71 | 5.08 | 4.83 | 4.85 | 4.68 | 4.85 | 4.69 | 4.84 | 4.68 |
| 9 | 5.21 | 5.09 | 5.45 | 5.04 | 5.52 | 5.08 | 5.39 | 5.00 | 5.39 | 5.00 | 5.38 | 4.99 |
| 10 | 4.18 | 4.74 | 5.60 | 5.12 | 5.59 | 5.12 | 5.53 | 5.08 | 5.53 | 5.08 | 5.52 | 5.07 |
| 11 | 3.15 | 4.31 | 5.46 | 5.05 | 5.38 | 5.00 | 5.38 | 5.00 | 5.39 | 5.00 | 5.37 | 4.99 |
| 12 | 2.22 | 3.82 | 5.14 | 4.86 | 4.99 | 4.77 | 5.05 | 4.80 | 5.05 | 4.80 | 5.03 | 4.79 |
| 13 | 1.48 | 3.32 | 4.69 | 4.59 | 4.49 | 4.47 | 4.59 | 4.53 | 4.59 | 4.53 | 4.58 | 4.52 |
| 14 | 1.00 | 2.85 | 4.19 | 4.28 | 3.95 | 4.13 | 4.09 | 4.22 | 4.09 | 4.22 | 4.08 | 4.21 |
| 15 | 0.83 | 2.48 | 3.69 | 3.96 | 3.42 | 3.78 | 3.59 | 3.90 | 3.59 | 3.89 | 3.59 | 3.89 |
| 16 | 0.83 | 2.24 | 3.23 | 3.65 | 2.94 | 3.44 | 3.14 | 3.59 | 3.14 | 3.58 | 3.13 | 3.58 |
| 17 | 0.83 | 2.06 | 2.84 | 3.37 | 2.54 | 3.15 | 2.75 | 3.31 | 2.75 | 3.30 | 2.75 | 3.30 |
| 18 | 0.83 | 1.93 | 2.51 | 3.12 | 2.22 | 2.90 | 2.43 | 3.07 | 2.43 | 3.06 | 2.43 | 3.06 |
| 19 | 0.83 | 1.84 | 2.23 | 2.91 | 1.96 | 2.68 | 2.17 | 2.86 | 2.16 | 2.85 | 2.16 | 2.85 |
| 20 | 0.83 | 1.78 | 2.00 | 2.72 | 1.75 | 2.50 | 1.94 | 2.67 | 1.94 | 2.67 | 1.94 | 2.67 |
| 21 | 0.83 | 1.73 | 1.81 | 2.56 | 1.58 | 2.35 | 1.76 | 2.52 | 1.76 | 2.51 | 1.76 | 2.51 |
| 22 | 0.83 | 1.69 | 1.65 | 2.42 | 1.44 | 2.22 | 1.61 | 2.38 | 1.60 | 2.38 | 1.61 | 2.38 |
| 23 | 0.83 | 1.67 | 1.51 | 2.30 | 1.33 | 2.12 | 1.48 | 2.26 | 1.48 | 2.26 | 1.48 | 2.26 |
| 24 | 0.83 | 1.65 | 1.40 | 2.19 | 1.23 | 2.03 | 1.37 | 2.16 | 1.37 | 2.16 | 1.37 | 2.16 |
| 25 | 0.83 | 1.64 | 1.30 | 2.10 | 1.16 | 1.95 | 1.28 | 2.07 | 1.28 | 2.07 | 1.28 | 2.07 |
| 26 | 0.83 | 1.63 | 1.22 | 2.02 | 1.10 | 1.89 | 1.20 | 2.00 | 1.20 | 1.99 | 1.20 | 1.99 |
| 27 | 0.83 | 1.62 | 1.15 | 1.95 | 1.05 | 1.84 | 1.14 | 1.93 | 1.14 | 1.93 | 1.14 | 1.93 |
| 28 | 0.83 | 1.61 | 1.10 | 1.89 | 1.01 | 1.80 | 1.08 | 1.87 | 1.08 | 1.87 | 1.09 | 1.87 |
| 29 | 0.83 | 1.61 | 1.05 | 1.84 | 0.98 | 1.76 | 1.04 | 1.83 | 1.04 | 1.82 | 1.04 | 1.82 |
| 30 | 0.83 | 1.61 | 1.01 | 1.79 | 0.95 | 1.73 | 1.00 | 1.79 | 1.00 | 1.78 | 1.00 | 1.78 |
| 31 | 0.83 | 1.61 | 0.98 | 1.76 | 0.93 | 1.71 | 0.97 | 1.75 | 0.97 | 1.75 | 0.97 | 1.75 |
| 32 | 0.83 | 1.60 | 0.95 | 1.73 | 0.91 | 1.69 | 0.94 | 1.72 | 0.94 | 1.72 | 0.94 | 1.72 |
| 33 | 0.83 | 1.60 | 0.93 | 1.70 | 0.90 | 1.67 | 0.92 | 1.70 | 0.92 | 1.70 | 0.92 | 1.70 |
| 34 | 0.83 | 1.60 | 0.91 | 1.68 | 0.89 | 1.66 | 0.91 | 1.68 | 0.90 | 1.68 | 0.90 | 1.68 |
| 35 | 0.83 | 1.60 | 0.89 | 1.67 | 0.88 | 1.65 | 0.89 | 1.66 | 0.89 | 1.66 | 0.89 | 1.66 |

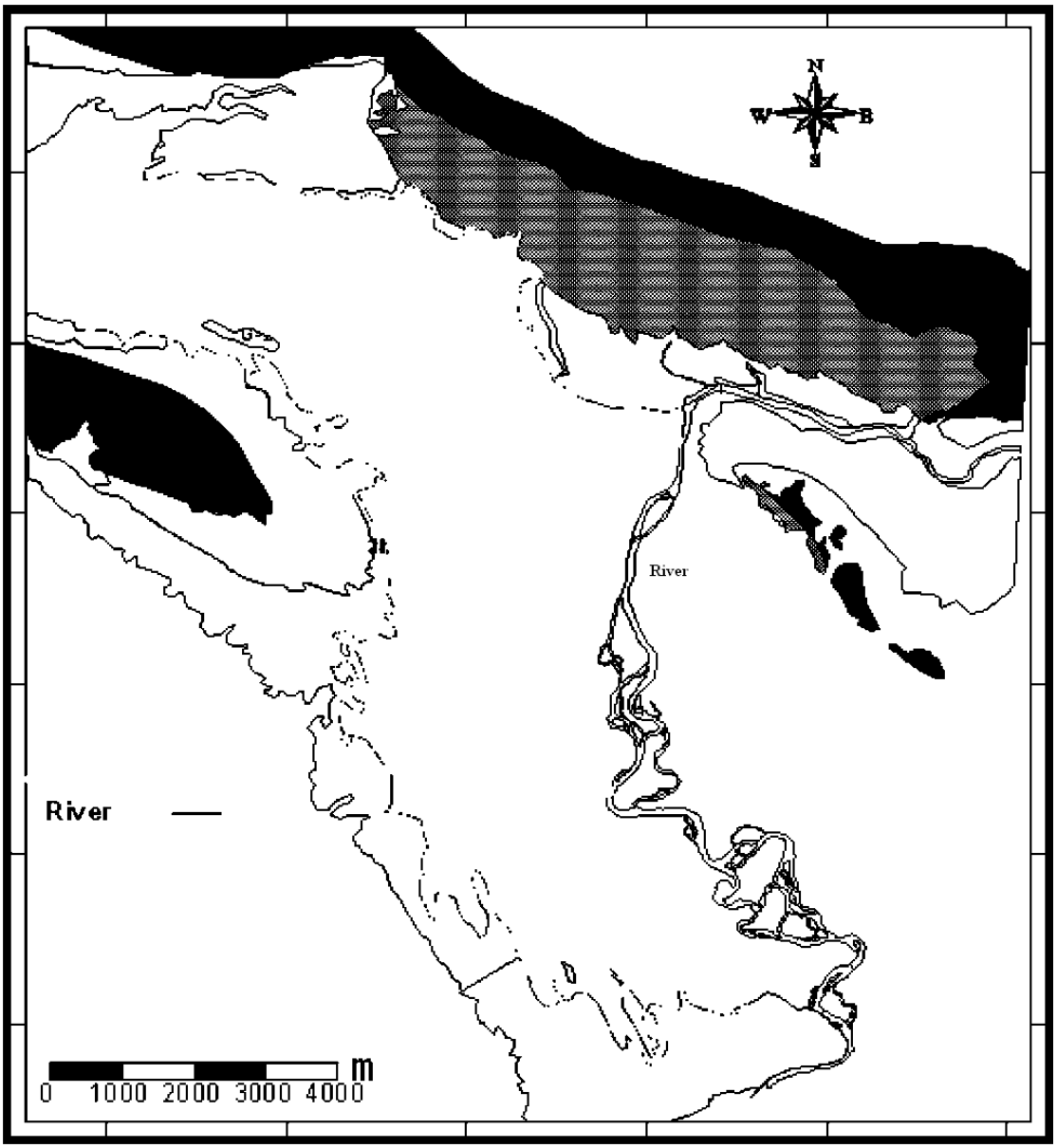


**Fig.1** A map of location and streams of Persian Gulf drainage basins

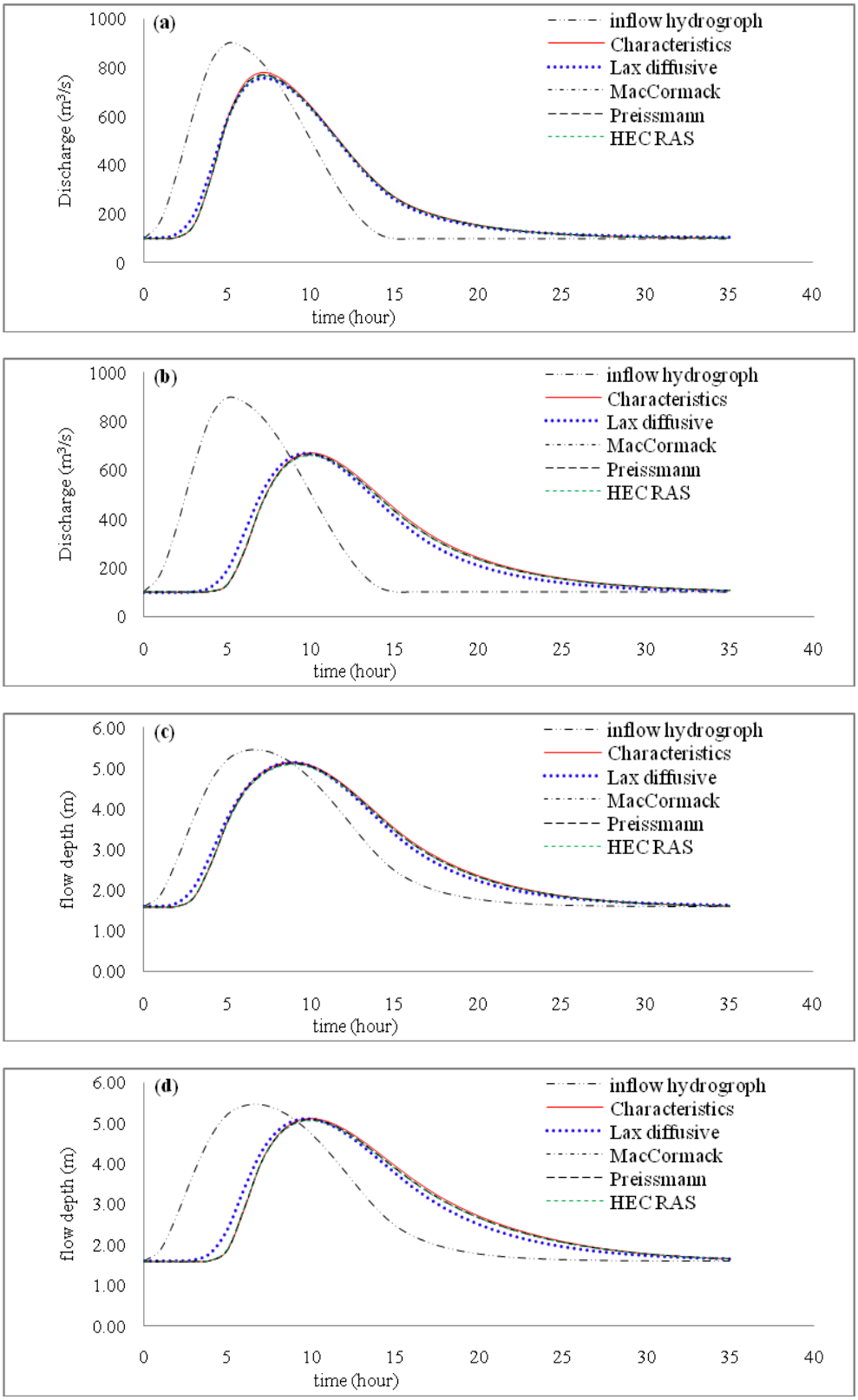


**Fig. 2** Simulation results of flow routing in the channel: (**a**) discharge hydrograph at 15 km, (**b**) discharge hydrograph at downstream-end, (**c**) stage hydrograph at 15 km (**d**) stage hydrograph at downstream end